THE JOURNAL OF BIOLOGICAL CHEMISTRY VOL. 286, NO. 36, pp. 31136–31144, September 9, 2011

The Atypical Two-component Sensor Kinase Lpl0330 from *Legionella pneumophila* Controls the Bifunctional Diguanylate Cyclase-Phosphodiesterase Lpl0329 to Modulate Bis-(3′-5′)-cyclic Dimeric GMP Synthesis[S]

Received for publication, February 15, 2011, and in revised form, July 5, 2011 Published, JBC Papers in Press, July 13, 2011, DOI 10.1074/jbc.M111.231340

Mélanie Levet-Paulo[1], Jean-Claude Lazzaroni, Christophe Gilbert, Danièle Atlan, Patricia Doublet, and Anne Vianney[2]

From the Université de Lyon, Université Lyon 1, CNRS UMR5240 "Microbiologie, Adaptation et Pathogénie," 69622 Villeurbanne, France

A significant part of bacterial two-component system response regulators contains effector domains predicted to be involved in metabolism of bis-(3′-5′)-cyclic dimeric guanosine monophosphate (c-di-GMP), a second messenger that plays a key role in many physiological processes. The intracellular level of c-di-GMP is controlled by diguanylate cyclase and phosphodiesterases activities associated with GGDEF and EAL domains, respectively. The *Legionella pneumophila* Lens genome displays 22 GGDEF/EAL domain-encoding genes. One of them, *lpl0329*, encodes a protein containing a two-component system receiver domain and both GGDEF and EAL domains. Here, we demonstrated that the GGDEF and EAL domains of Lpl0329 are both functional and lead to simultaneous synthesis and hydrolysis of c-di-GMP. Moreover, these two opposite activities are finely regulated by Lpl0329 phosphorylation due to the atypical histidine kinase Lpl0330. Indeed, Lpl0330 was found to autophosphorylate on a histidine residue in an atypical H box, which is conserved in various bacteria species and thus defines a new histidine kinase subfamily. Lpl0330 also catalyzes the phosphotranfer to Lpl0329, which results in a diguanylate cyclase activity decrease whereas phosphodiesterase activity remains efficient. Altogether, these data present (i) a new histidine kinase subfamily based on the conservation of an original H box that we named HGN H box, and (ii) the first example of a bifunctional enzyme that modulates synthesis and turnover of c-di-GMP in response to phosphorylation of its receiver domain.

Two-component regulatory systems (TCSs)[3] were the first major mode of signal transduction identified in bacteria. These systems couple a broad range of external or internal signals to regulation of diverse fundamental processes, such as metabolism, motility, and virulence (1–3). Typical TCSs are composed of a sensor histidine kinase (HK) and a response regulator protein (RR) usually encoded by a pair of adjacent genes. Both the HK and the RR are multidomain proteins. The N termini of HKs are diverse and usually contain sensory or "input" domains that respond to environmental stimuli to activate the transmitter domain. The transmitter domain consists of two distinct subdomains: an ATP-binding HATPase domain involved in the autophosphorylation of the HK at the conserved histidine residue in a His-containing phosphoacceptor (dimerization) His kinase A (HisKA) domain (4). The phosphoryl group is then transferred from this histidine residue to an aspartate residue in the receiver domain of the RR partner. This phosphorylation activates C-terminal effector or "output" domain of RR, which executes an appropriate cellular response. The majority of RR effectors are nucleic acid binding domains acting as transcriptional regulators. The remaining RRs contain domains that can be categorized in enzymatic, stand alone, or protein/ligand binding domains (3). A significant part of the RRs containing enzymatic domains (6% of all RRs) are found in proteins involved in the biosynthesis of cyclic dimeric GMP (c-di-GMP), highlighting the relationship between TCSs and the c-di-GMP cellular level.

c-di-GMP is an ubiquitous second messenger that has emerged as a key player in bacterial signaling. Actually, it was found to regulate main functions such as biofilm formation, virulence, motility, differentiation, and cell-cell signaling (5) and was recently shown to control an original "flagellar brake" mechanism (6–8). Proteins involved in the metabolism of c-di-GMP exhibit GGDEF and/or EAL domains responsible for the synthesis and hydrolysis of this secondary metabolite, via their diguanylate cyclase (DGC) and phosphodiesterase (PDE) activities, respectively.

The majority of sequenced bacterial genomes encode more than one gene encoding GGDEF/EAL proteins, and they are particularly expanded in gamma proteobacteria with a median of 22 genes/genome (9). This had led to the question on how the activities of these different GGDEF or EAL proteins are regulated. A first level of regulation resides in transcriptional regulation. Most of the 28 GGDEF/EAL domain-encoding genes in

[S] The on-line version of this article (available at http://www.jbc.org) contains supplemental Fig. S1.

[1] Supported by a fellowship from the Ministère de l'Enseignement Supérieur et de la Recherche.

[2] To whom correspondence should be addressed: UMR 5240, bât. Lwoff (R+3), 10 rue Dubois, 69622 Villeurbanne, France. Fax: 33-4-72-43-26-86; E-mail: anne.vianney@univ-lyon1.fr.

[3] The abbreviations used are: TCS, two-component regulatory system; AcP, acetyl phosphate; CDD, NCBI Conserved Domain Data base; c-di-GMP, bis-(3′-5′)-cyclic dimeric guanosine monophosphate; DGC, diguanylate cyclase; HK, histidine kinase; PAS, Per-Arnt-Sim; PDE, phosphodiesterase; REC, receiver; RR, response regulator; GTPαS, guanosine 5′-O-thiotriphosphate; HisKA, histidine kinase A domain; PEI, polyethyleneimine.

TABLE 1
DNA sequences of oligonucleotides used in this study
Italic letters indicate the sites where point mutations have been introduced. Underlined letters indicate the recognition sites for restriction enzymes.

Oligonucleotides	Primer sequence (5′ to 3′)
Plasmid constructs	
329	TTGAGTACGA*GGATCC*ATGAGTACTGAATC
329R	TGCAATCC*GTCGAC*TAGCTCTTGTAGATG
330	TTGACAG*GATCC*CATCGGTTGTTGCAGCGACAG
330R	AAGATT*GTCGAC*TACTCATTTCTACCTCGTACTC
Substitution in Lpl0329	
D87N	CCATACCCACTCGCCTTTGTTAACATAAGAATGCCC
	GGGCATTCTTATGTTAACAAAGGCGAGTGGGTATGG
E396K F397L	CCAGACTTGGTGGGGATAAGCTTGTAATGCTTTTTCAATCG
	CGATTGAAAAAGCATTACAAGCTTATCCCCACCAAGTCTGG
W526S	CCATGGAAGCATTAATCCGATCGAATCACCCGCAAAAAGG
	CCTTTTTGCGGGTGATTCGATCGGATTAATGCTTCCATGG
Substitution in Lpl0330	
H186N	GGAAAATTATTGAAGAGCAAGTTAACGAACTGAATAATAAACTGGTTTCAACAG
	CTGTTGAAACCAGTTTATTATTCAGTTC*GTTA*ACTTGCTCTTCAATAATTTTCC
H234N	GCCATTATTCTGAAAAAGAATATATCCAACATTAATTATAAAAAACTGTCCGC
	GCGGACAGTTTTTTATAA*TTA*ATGTTGGATATATTCTTTTTCAGAATAATGGC
H210N	GAAGTAGCCACCTCGATACTTAATAATGTGGGCAATATATTAAACAG
	CTGTTTAATATATTGCCCACA*T*TATTAAGTATCGAGGTGGCTACTTC

Escherichia coli are expressed during entry into stationary phase, with 15 being under sigma S control (10). In *Legionella pneumophila*, 18 of the 24 GGDEF/EAL domain-encoding genes are up-regulated in transmission phase, the extracellular stationary phase (11). Given that many proteins are expressed under the same condition, their spatial control and post-translational regulation must be also critical as suggested by the variety of sensory domains associated with these proteins, consistent with multiple signal input in an extra-host environment (9, 12). However, the question remains what determines the overall activity of hybrid proteins that contain both GGDEF and EAL domains and thus present a "biochemical conundrum" (13). In many cases, only one of the GGDEF or EAL domain seems to be catalytically active (5). Nevertheless, three proteins showing both activities have been identified, so far raising question on how the two activities are reciprocally regulated: MSDGC-1 in *Mycobacterium smegmatis* (14), BphG1 in *Rhodobacter sphaeroides* (15), and ScrC in *Vibrio parahemeolyticus* (14–16). It was proposed that these proteins could switch between states that are able to synthesize and hydrolyze c-di-GMP (13). Thus, the interaction between ScrC and two accessory proteins, ScrA and ScrB, influences the balance between DGC and PDE activities of ScrC in *V. parahemeolyticus* (16). Furthermore, the DGC (but not PDE) activity of BphG1 is light-dependent in *R. sphaeroides* (15).

In *L. pneumophila* Lens genome, two adjacent genes *lpl0329* and *lpl0330* encode a putative RR with both GGDEF and EAL domains, and a putative HK, respectively. Here, we demonstrated that Lpl0330 and Lpl0329 form a functional TCS. Actually, the HK Lpl0330 autophosphorylates although it contains none of the four HisKA domains listed in the Pfam data base (17). The phosphoacceptor histidine residue in Lpl0330 was identified and was found to be conserved in numerous HKs of various bacterial species, leading us to propose a new HisKA domain. Our results also showed that phosphotransfer from Lpl0330 to Lpl0329 occurs. Moreover, Lpl0329 has been characterized as a RR with two opposite activities: GGDEF and EAL domains of Lpl0329 are both functional *in vitro* and lead to simultaneous synthesis and hydrolysis of c-di-GMP. Finally, we observed for the first time that DGC activity depends on the phosphorylation state of a DGC/PDE enzyme, suggesting a "molecular switch" that favors one of the two-enzymatic activities and affects the production rate of c-di-GMP.

EXPERIMENTAL PROCEDURES

Bacterial Strains and Growth Conditions—E. coli DH5α was used for DNA cloning. *E. coli* strain BL21 (DE3), used for recombinant protein overproductions, carries plasmid pREP4-*groESL* which harbors *groES groEL* genes encoding two chaperone proteins. *E. coli* strains were grown at 37 °C in Luria Broth (LB) supplemented with antibiotics for selection, when necessary (ampicillin 100 μg/ml, kanamycin 25 μg/ml). *L. pneumophila* strain Lens was used for preparing genomic DNA. It was grown at 30 °C on buffered charcoal yeast extract.

Overproduction of Lpl0329 and Lpl0330—Plasmid pQE30 (Qiagen) was used for production of *L. pneumophila* Lpl0329 and Lpl0330 proteins with His_6 tag fusion. The *lpl0329* and *lpl0330* coding regions (corresponding to the 1–740 and 5–471 amino acids) were PCR-amplified using *L. pneumophila* Lens chromosomal DNA as template and the primers 329 and 329R (for *lpl0329*) and 330 and 330R (for *lpl0330*), with sequence modifications introduced to create BamHI/SalI restriction sites (Table 1). The amplified DNA fragments were digested by BamHI and SalI and then inserted into pQE30 digested by the same enzymes. The resulting constructs pQE30-His_6-Lpl0329 and pQE30-His_6-Lpl0330 were transformed into *E. coli* BL21 (pREP4-*groESL*). The resulting strains were grown in LB medium with ampicillin and kanamycin at 37 °C, and expression was induced at 20 °C by adding 1 mM isopropyl-β-D-thiogalactopyranoside at A_{600} 0.6–0.8.

Purification of Recombinant Proteins—The BL21 (pREP4-*groESL*) cells harboring His_6-Lpl0329 and His_6-Lpl0330 were harvested by centrifugation (6000 × *g*, 10 min, 4 °C), washed in buffer A (50 mM Tris, pH 7.5, 150 mM NaCl, 10 mM imidazole, 1 mM β-mercaptoethanol, 1 mM EDTA) and disrupted in a French press cell. The suspension was cleared by centrifugation. Supernatant was incubated 1 h at 4 °C with Ni-nitrilotriacetic acid

affinity resin (Qiagen) and loaded onto a polypropylene column (Qiagen). Resin was washed with buffer A containing 20 mM imidazole, and His_6-tagged proteins were eluted with buffer A containing 150 mM imidazole. The lysates, column washes, and elutions were analyzed by SDS-PAGE and Coomassie Brilliant Blue staining to access protein purity. Fractions containing pure proteins were pooled and dialyzed against reaction buffer. The concentrations of the dialyzed protein fractions were determined using Nanodrop 2000 (Thermo).

Amino Acid Substitutions in Lpl0329 and in Lpl0330—Substitutions in *lpl0329* and *lpl0330* were performed with a QuikChange™ II Site-directed Mutagenesis kit (Stratagene) using the primers listed in Table 1 and pQE30-His_6-Lpl0329 or pQE30-His_6-Lpl0330 as template. Final constructs were used to transform *E. coli* BL21 (pREP4-*groESL*).

In Vitro Autophosphorylation Assays—Purified His_6-Lpl0330, His_6-Lpl0330H186N, or His_6-Lpl0330H210N (5 μM) was incubated with 0.2 mM ATP and 100 nM [γ-^{32}P]ATP (3000 Ci/mmol) (PerkinElmer Life Sciences) at 30 °C, in a final volume of 25 μl in phosphorylation buffer (50 mM Tris, pH 7.5, 150 mM NaCl) supplemented separately with $MgCl_2$, $MnCl_2$, and $CaCl_2$, at a final concentration of 20 mM. Aliquots were removed at different time intervals, and the reactions were stopped by the addition of 2 × SDS-PAGE loading buffer and analyzed by 12% SDS-PAGE. The gels were subjected to autoradiography and analyzed by phosphorimaging.

In Vitro Phosphotransfer Assay—Phosphotransfer reactions from Lpl0330 to Lpl0329 were performed as described by Fritsch *et al*. (18). In brief, His_6-Lpl0330 (2.8 μM) was incubated for 15 min at 30 °C in reaction buffer (50 mM Tris, pH 7.5, 150 mM NaCl, 20 mM $MgCl_2$) containing 100 nM [γ-^{32}P]ATP (3000 Ci/mmol) (PerkinElmer Life Sciences), and the phosphotransfer reaction was initiated by the addition of the RR proteins, His_6-Lpl0329 or His_6-Lpl0329 D87N (3 μM). Reactions were stopped with 2 × SDS-PAGE loading buffer supplemented with 50 mM Na_2EDTA, and analyzed by 12% SDS-PAGE. The gels were subjected to autoradiography and analyzed by phosphorimaging.

DGC and PDE Assays and TLC Analysis—DGC and PDE assays were adapted from procedures described by others (19, 20). Purified His_6-Lpl0329, His_6-Lpl0329W526S, or His_6-Lpl0329E396K, F397L (5 μM) was incubated in reaction buffer (described previously) with 50 μM GTP and 15 μCi of [α-^{32}P]GTP (PerkinElmer Life Sciences) in a final volume of 50 μl. Aliquots were withdrawn at regular time intervals, and the reaction was stopped by the addition of 0.3 volume of 0.5 M EDTA, pH 8. Lpl0329 phosphorylation by acetylphosphate (AcP) was achieved as described previously (21–23) by incubating the proteins in the reaction buffer supplemented with 25 mM AcP (Sigma-Aldrich) at 30 °C for 2 h prior to enzymatic assay. Reaction products (1.5 μl) were separated on PEI-cellulose plates (Macherey Nagel) in 1:1.5 (v/v) 4 M $(NH_4)_2SO_4$, pH 3.6, and 1.5 M KH_2PO_4, pH 3.6. Plates were exposed to a phosphorimager screen. The intensity of the various radioactive species was calculated by quantifying the intensities of the relevant spots using Optiquant software. A two-tailed Student's *t* test was used to analyze the data. *p* values of < 0.05 were considered significant.

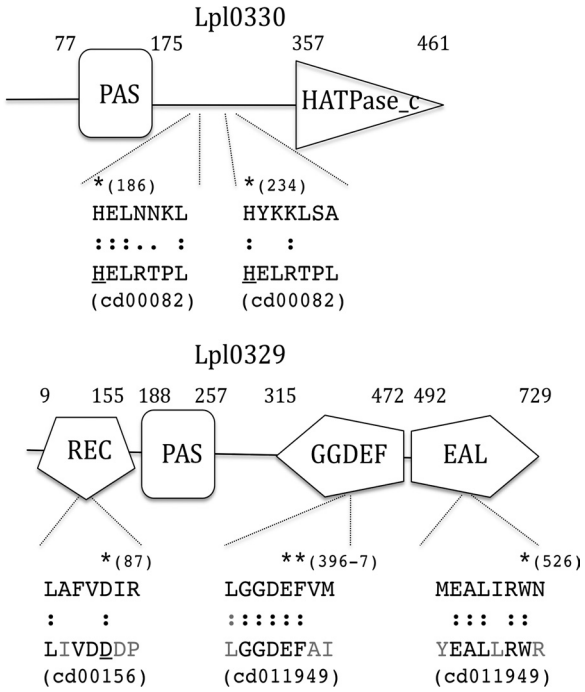

FIGURE 1. **Schematic diagram of conserved domains detected by NCBI CDD (26) in Lpl0330 and Lpl0329.** The amino acid positions where the predicted domains start and end are shown. PAS domain of Lpl0330 contains a putative heme pocket. HATPase_c, ATP binding and hydrolysis catalytic domain; GGDEF, putative diguanylate cyclase domain; EAL, putative phosphodiesterase domain. Relevant segments of sequence alignment between Lpl0329 or Lpl0330 sequences (*top*) and consensus domains from CDD (*bottom*) are shown, with position-specific scoring matrix identifier (26) listed between *parentheses*. Phosphorylation sites of the consensus HisKA domain (cd00082) and REC domain (cd00156) are *underlined*. Conserved amino acids residues in consensus sequences are in *black*. Amino acid residues exchanged are indicated with one star (*) with exact positions listed between *parentheses*. *Double points* indicate amino acid residues that are identical in 100% of consensus sequences.

RESULTS

Domain Architecture of Lpl0330 and Lpl0329—Development of genomics led to massive identification of TCSs in microbial genomes and family assignments of HKs and RRs based on their domain architecture (24, 25). The HK transmitter domain consists typically of two distinct domains: a well conserved C-terminal catalytic and ATP binding domain, also known as HATPase_c in the NCBI Conserved Domain Data base (CDD) or Pfam data base (17, 26) and a less-conserved dimerization and histidine phosphotransfer (DHp) domain, referred as the HisKA domain in CDD and Pfam data base; the Pfam data base identifies four distinct HisKA domains, namely HisKA (PF00512), HisKA_2 (PF07568), HisKA_3 (PFO7730), and HWE_HK (PF07536). Lpl0330 contains a conserved HATPase_c ATP binding catalytic domain (CDD expect value = 7.89 e^{-12}) but lacks a conserved HisKA phosphorylation/dimerization domain (Fig. 1). So, Lpl0330 is a histidine kinase homolog without a conserved phosphoacceptor His residue. However, local sequence alignment with the main HisKA domain (cd0082 or PF00512) led us to identify His-186 as a putative phosphorylation site (Fig. 1). The N-terminal Per-Arnt-Sim (PAS) domain of Lpl0330 (CDD expect value = 2.09 e^{-04}) contains a putative heme pocket. Besides, Lpl0330 homologs in Philadelphia and Corby *L. pneumophila* genomes

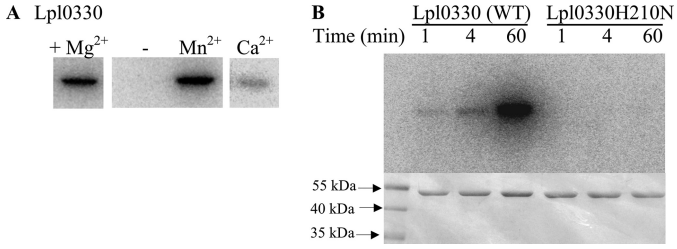

FIGURE 2. *A*, autophosphorylation of His_6-Lpl0330. 5 μM purified His_6-Lpl0330 was incubated at 30 °C with [γ-^{32}P]ATP for 60 min in the presence of Mg^{2+} and 60 min in the presence or not (−) of Ca^{2+} or Mn^{2+}. All samples were subjected to 12% SDS-PAGE and exposed to a phosphorimager screen. *B*, His-210 is required for Lpl0330 phosphorylation. 5 μM purified His_6-Lpl0330 and His_6-Lpl0330H210N were incubated at 30 °C with [γ-^{32}P]ATP for 1, 4, or 60 min in the presence of Mg^{2+}. All samples were subjected to 12% SDS-PAGE, stained with Coomassie Blue (*bottom panel*), and exposed to a phosphorimager screen (*top panel*).

were annotated as FixL, in reference to the well studied *Rhizobium meliloti* oxygen-sensing histidine kinase (27).

On the other hand, the prototypical RR contains a N-terminal receiver (REC) domain linked to a variable C-terminal effector domain. Lpl0329 is a RR homolog consisting of a REC domain (CDD expect value = 7.90 e^{-08}) followed by a PAS domain (CDD expect value = 6.27 e^{-03}), a GGDEF domain (CDD expect value = 2.51 e^{-55}), and an EAL domain (CDD expect value = 4.64 e^{-72}) (Fig. 1).

Lpl0330 Autophosphorylates in Vitro—To determine whether Lpl0330 autophosphorylates *in vitro*, His_6-tagged Lpl0330 was overproduced and purified to near homogeneity by nickel affinity chromatography. Phosphorylation of purified His_6-Lpl0330 was assessed in the presence of [γ-^{32}P]ATP by using a standard kinase assay. His_6-Lpl0330 was radioactively labeled when incubated in the presence of divalent cations $MgCl_2$, $MnCl_2$, or to a lesser extent, $CaCl_2$ (Fig. 2*A*). These results indicate that Lpl0330 possesses a autokinase activity and requires Mg^{2+} or Mn^{2+} as cofactor for autophosphorylation.

Lpl0330 Is a Member of a New HK Subfamily—The HK Lpl0330 autophosphorylates despite the lack of a conserved HisKA domain. Indeed, it does not contain any of the four HisKA domains listed in the Pfam data base, namely HisKA (PF00512), HisKA_2 (PF07568), HisKA_3 (PF07730), and HWE_HK (PF07536) (17). However, sequence alignments with residues near the phosphorylation site of the major consensus HisKA domain (PF00512) identified His-186 as a potential phosphorylation site (Fig. 1). Another histidine residue, namely His-234, is followed by a conserved basic residue in the third position, which argues for a putative phosphoacceptor site in histidine kinases (28) (Fig. 1). His-186 and His-234 were substituted to Asn residue by site-directed mutagenesis, and the resulting proteins, His_6-Lpl0330H186N and His_6-Lpl0330H234N, were purified and then assayed for autophosphorylation. Autoradiography showed that His_6-Lpl0330H186N and His_6-Lpl0330H234N were radioactively labeled as the wild-type protein and slightly less than the wild type, respectively, thus demonstrating that neither His-186 nor His-234 is the phophoacceptor on Lpl0330 (supplemental Fig. S1).

To investigate the phosphorylation site of Lpl0330 further, related proteins were searched by using the inter PAS-HATPase_c domains sequence of Lpl0330 as a query in BLAST (29). Interestingly, 64 other histidine kinases from a variety of bacteria species were identified (Fig. 3*A*). Alignments highlighted a major conserved region including a His residue (His-210 for Lpl0330) followed by a N-V/I-G-N motif (Fig. 3*A*). The formatted logo shows several well conserved residues upstream from the His residue drawing a G-*X*-*X*-E-*X*-A-*X*-*X*-*X*-L motif, but also some conserved residues further downstream that could be taken into consideration to define a new HisKA domain (Fig. 3*B*). Site-directed mutagenesis was performed to replace His-210 with Asn-210. *In vitro* phosphorylation assays of the purified Lpl0330H210N demonstrated that this substitution results in the absence of autophosphorylation (Fig. 2*C*). So, the His-210 residue of the HK Lpl0330 is most likely the phosphoacceptor site, and the conserved motif identified by sequence alignment of 65 atypical HK defines a new H box that we named HGN on the basis of the presence of these three conserved residues in all sequences. It is noteworthy that the HGN H box has low similarity with H boxes from all other known HK types (30) (Fig. 3*C*). Moreover, all of the proteins containing the HGN H box were characterized by an HATPase catalytic domain lacking identified HisKA domain. Thus, the HGN H box belongs to a new HisKA domain which characterizes a new subfamily of histidine kinases.

Asp-87 of Lpl0329 Is Unstably Phosphorylated by Lpl0330—Lpl0329 was predicted to be the response regulator of the Lpl0329-Lpl0330 TCS. More precisely, the conserved Asp-87 in the Lpl0329 REC domain was identified as the putative phosphorylation target of Lpl0330 (Fig. 1). To confirm this prediction, we overproduced and purified the recombinant proteins His_6-Lpl0329 and His_6-Lpl0329D87N, with Asp-87 replaced by Asn by site-directed mutagenesis. *In vitro* phosphorylation assays with the purified recombinant proteins were performed. As described above, incubation of His_6-Lpl0330 in the presence of [γ-^{32}P]ATP resulted in the autophosphorylation of the HK (Fig. 4*A*), whereas His_6-Lpl0329 and His_6-Lpl0329D87N were not autophosphorylated in these conditions (data not shown). When His_6-Lpl0330 and His_6-Lpl0329 were combined, complete dephosphorylation of His_6-Lpl0330-P was observed, probably due to the phosphoryl group transfer to it of substrate His_6-Lpl0329. However, the phosphorylated form of His_6-Lpl0329 did not accumulate to significant levels. It is noteworthy that His_6-Lpl0330 phosphorylation is still detected in the presence of His_6-Lpl0329D87N (Fig. 4*A*). These results support that Lpl0330 is able to transfer its phosphate on the Asp-87 residue of Lpl0329 and that the half-life of the Lpl0329 phosphorylated form (P∼Lpl0329) could be too short to allow its detection, as previously reported for other TCSs (18, 31, 32). Finally, phosphorylated His_6-Lpl0329 could only be detected within the first 120 s of incubation at room temperature upon its addition to His_6-Lpl0330, which was pretreated with [γ-^{32}P]ATP for 15 min (Fig. 4*B*), as described previously (18). Moreover, the phosphorylation site of Lpl0329 is the predicted Asp-87, as His_6-Lpl0329D87N was no more radioactively labeled (Fig. 4*B*). Together, our results clearly indicate that phosphotransfer actually occurs between Lpl0330 and the Asp-87 residue of Lpl0329.

Lpl0329 Is a DGC/PDE Bifunctional Enzyme—Lpl0329 harbors both GGDEF and EAL domains described to trigger the

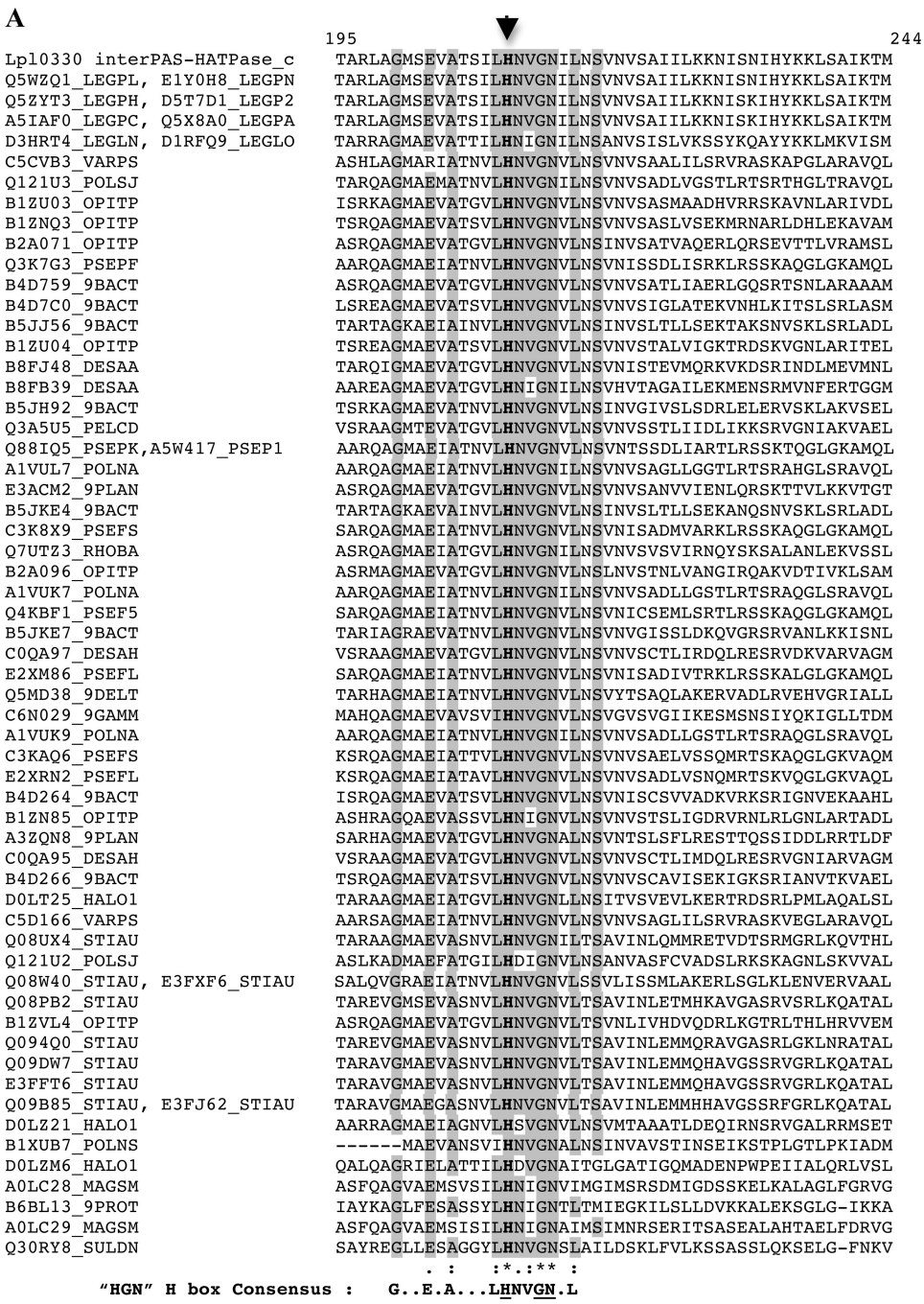

FIGURE 3. *A*, amino acid sequence alignment of portion of the inter-PAS-HATPase_c region of Lpl0330 defines a new HK subfamily. The 65 predicted histidine kinases identified by BLAST with the inter-PAS-HATPase sequence of Lpl0330 as the query were aligned by ClustalW (44). Only the sequences encompassing the putative H boxes are shown. The *closed arrowhead* identifies the histidine predicted to form the phosphohistidine intermediate. *Gray boxes* denote conserved amino acids. Identical residues in the 65 sequences are *underlined* in the consensus sequence. The residue numbers are for Lpl0330 (Q5WZQ1_LEGPL). Sequences accession number are listed (Uniprot knowledgebase, UniprotKB). To simplify the alignment, proteins with the same local sequence are pooled on the same line. Sequences are from *L. pneumophila* (*LEGP*), *Legionella longbeachae* (*LEGL*), *Legionella drancourtii* (*9GAMM*), *Pseudomonas fluorescens* (*PSEPF*), *Pseudomonas putida* (*PSEP*), *Variovorax paradoxus* (*VARPS*), *Polaromonas* sp. (*POLSJ*), *Polaromonas naphthalenivorans* (*POLNA*), *Polynucleobacter necessarius* (*POLNS*), *Stigmatella aurantiaca* (*STIAU*), *Cystobacter fuscus* (*9DELT*), *Haliangium ochraceum* (*HALO1*), *Desulfatibacillum alkenivorans* (*DESAA*), *Desulfobacterium autotrophicum* (*DESAH*), *Pelobacter carbinolicus* (*PELCD*), *Sulfurimonas denitrificans* (*SULDN*), *Magnetococcus* sp. (*MAGSM*), *Opitutus terrae* (*OPITP*), *Verrucomicrobiae bacterium*, *Chthoniobacter flavus* (*9BACT*), *Rhodopirellula baltica* (*RHOBA*), *Planctomyces brasiliensis, Blastopirellula marina* (*9PLAN*). *B*, sequence logo of the H box region of the HGN HK subfamily. Sequence logo was generated using the WebLogo tool (45) from the multiple alignment above. Residue numbering starts from Thr-195 of the Lpl0330 sequence. *C*, amino acid sequence alignment of HGN H box with representative member of each of the 11 HK subfamilies described by Wolanin *et al.* (30). The proteins used to make this alignment and the residue positions are indicated in *parentheses*. His conserved proposed as phosphoacceptor site are shown *boxed*. *Gray boxes* denote conserved amino acids with the HGN H box.

biosynthesis and the degradation of c-di-GMP, respectively. To check whether these domains are functional, Lpl0329 was assayed for its ability to synthesize and/or degrade c-di-GMP *in vitro*. Purified His_6-Lpl0329 was incubated in the presence of [α-^{32}P]GTP, and reaction products were analyzed by TLC and phosphorimaging. All R_F values for nucleotide species detected in these assays

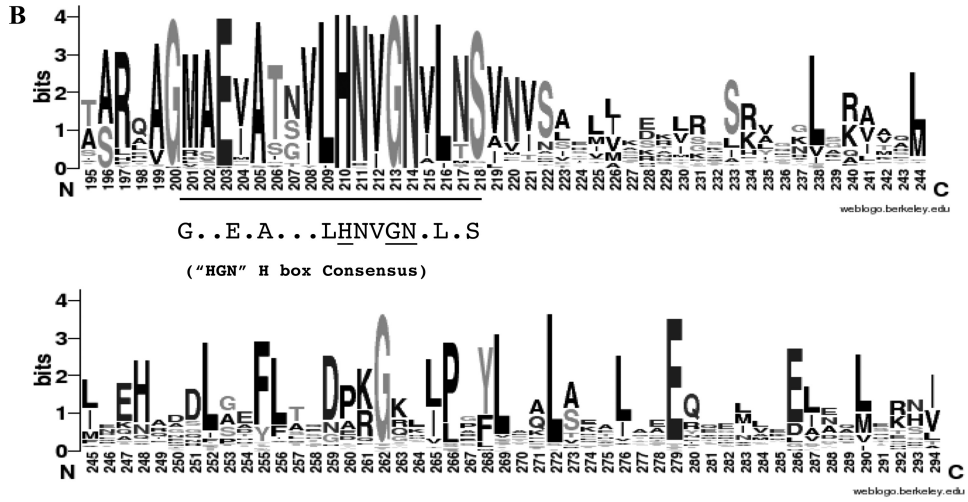

FIGURE 3—*continued*.

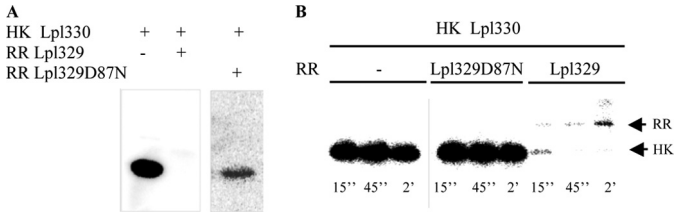

FIGURE 4. **Phosphotransfer of Lpl0330 to Lpl0329.** *A*, purified His_6-Lpl0330 (2 μM) and His_6-Lpl0329 (2 μM) or His_6-Lpl0329D87N (2 μM) were mixed and incubated for 30 min at 30 °C. [γ-^{32}P]ATP was added in the mixture. The reactions were stopped after 5 min by the addition of sample buffer, and reaction mixtures were subjected to 12% SDS-PAGE and exposed to a phosphorimager screen. *B*, purified His_6-Lpl0330 (2.8 μM) was incubated for 15 min at 30 °C in the presence of [γ-^{32}P]ATP and then His_6-Lpl0329 (3 μM) or His_6-Lpl0329D87N (3 μM) was added at room temperature. The reactions were stopped at the indicated time points by the addition of sample buffer, and reaction mixtures were subjected to 12% SDS-PAGE and exposed to a phosphorimager screen.

(Fig. 5*A*) agreed with those identified previously by Wan *et al.* (20). Clearly, His_6-Lpl0329 exhibits a DGC activity that synthesized c-di-GMP from GTP (Fig. 5*A*). However, c-di-GMP did not accumulate because it was rapidly converted into pGpG, demonstrating that Lpl0329 also possesses a PDE activity (Fig. 5*A*).

To confirm that these activities involve GGDEF and EAL domains, amino acid substitutions in highly conserved residues were introduced into Lpl0329 by site-directed mutagenesis. The resulting purified proteins were tested for DGC and PDE activities. As expected, E396K and F397L substitutions in GGDEF domain and W526S substitution in EAL domain abolished DGC and PDE activities, respectively (Fig. 5*A*).

Lpl0329 Phosphorylation Reduces Its DGC Activity—All of the results described above indicate that Lpl0330 (HK) and Lpl0329 (RR) constitute a functional TCS and that Lpl0329 is a bifunctional DGC/PDE enzyme. To investigate the role of phosphorylation on Lpl0329 activities, DGC and PDE assays were performed in vitro with both Lpl0329 and Lpl0330, in the absence or the presence of the phosphate donor ATP (necessary for phosphotransfer). The presence of ATP, and so the phosphorylation of Lpl0329, seemed to inhibit DGC activity slightly (data not shown). However, as described above, we could not check the phosphorylation state of Lpl0329 because of the very short P~Lpl0329 half-life. To circumvent the problem and given that many response regulators can autophosphorylate by using low molecular weight phosphate donors such as AcP (21–23, 33), the DGC and PDE activities of Lpl0329 were measured in the presence of this compound. The addition of AcP resulted in a decrease of the GTP consumption, thus suggesting that Lpl0329 phosphorylation negatively controlled DGC activity (Fig. 5*B2*). By contrast, PDE activity remained efficient and prevented c-di-GMP accumulation, especially during the early time of reaction (Fig. 5*B2*). To assess whether this decrease of DGC activity is due to a nonspecific inhibitory effect of AcP, the experiment was repeated with Lpl0329D87N mutant that cannot be phosphorylated (Fig. 5*C*). In the presence of AcP, a nonsignificant (p values > 0.12) inhibitor effect on DGC activity of Lpl0329D87N was observed, but this effect was clearly lower compared with the significant effect (p value < 0.0032) observed on the DGC activity of the wild-type protein (Fig. 5*C*). Thus, Lpl0329 phosphorylation could lead to a molecular switch that favors one of the two enzymatic activities, thus resulting in a fine control of the c-di-GMP concentration.

DISCUSSION

In this study, we highlighted an original mechanism of c-di-GMP biosynthesis regulation by a two-component system-type

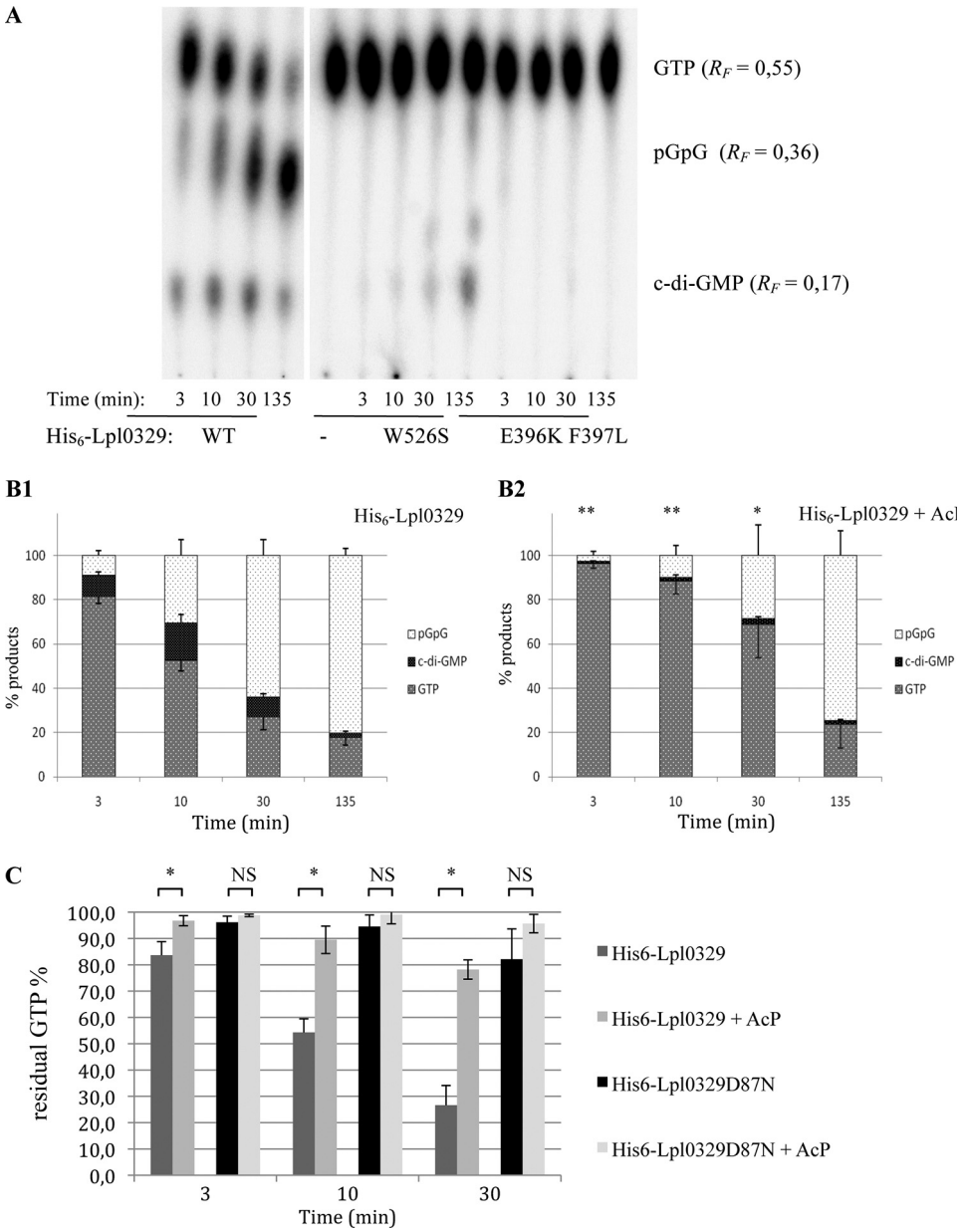

FIGURE 5. *A*, *L. pneumophila* Lpl0329 has both DGC and PDE activities which depend on GGDEF and EAL domains, respectively. Purified His_6-Lpl0329 (wild type or mutant as indicated) was incubated with [γ-^{32}P]-GTP, as described under "Experimental Procedures." Samples were withdrawn at different time points, analyzed on PEI-cellulose TLC, and plates were exposed to a phosphorimager screen. Amino acid mutations W526S in the EAL domain and E396K F397L in the GGDEF domain of His_6-Lpl0329 are indicated. GTP without protein was run as control (−). *B*, DGC activity after phosphorylation of Lpl0329 by AcP. Purified His_6-Lpl0329 was incubated for 2 h at 30 °C in the absence (*B1*) or presence (*B2*) of AcP. The reactions were performed with addition of [γ-^{32}P]GTP. Samples were withdrawn at different time points, analyzed on PEI-cellulose TLC, and plates were exposed to a phosphorimager screen allowing quantification of each radioactive product. The total label of each time reaction was considered 100%. *, $p < 0.05$ for comparison of GTP rate with or without AcP; **, $p < 0.05$ for comparison of c-di-GMP and GTP rates with or without AcP. *C*, specificity of the DGC inhibition by AcP. Purified His_6-Lpl0329 and His_6-Lpl0329D87N were incubated for 2 h at 30 °C in the absence or presence of AcP. The reactions were performed with the addition of [γ-^{32}P]GTP. Samples were withdrawn at different time points, analyzed on PEI-cellulose TLC, and plates were exposed to a phosphorimager screen allowing quantification of each radioactive product. GTP consumption by DGC activities is expressed as a percentage of remaining [γ-^{32}P]GTP. *, $p < 0.05$; *NS*, nonsignificant ($p > 0.05$), for comparison of GTP consumption with or without AcP.

phosphorylation. Indeed, we have shown that Lpl0329 is a bifunctional enzyme harboring both DGC and PDE activities, which are balanced by aspartate phosphorylation by the atypical HK Lpl0330.

Lpl0330 was found to autophosphorylate on a histidine residue in an atypical H box, namely the HGN H box. HisKA domains, which contain the H box with the phosphoryl-accepting His residue, are usually used to predict HK activities. It should be noted that the four HisKA domains currently described do not cover the full diversity of HKs, as some experimentally characterized sensory HKs contain domains that are not recognized by these profiles (4). The atypical HGN H box identified here defines a new histidine kinase subfamily and could be used to annotate new members of this family. Members of this family are retrieved in three phyla of bacteria, namely Verrucomicrobia, Planctomycetes, and Proteobacteria.

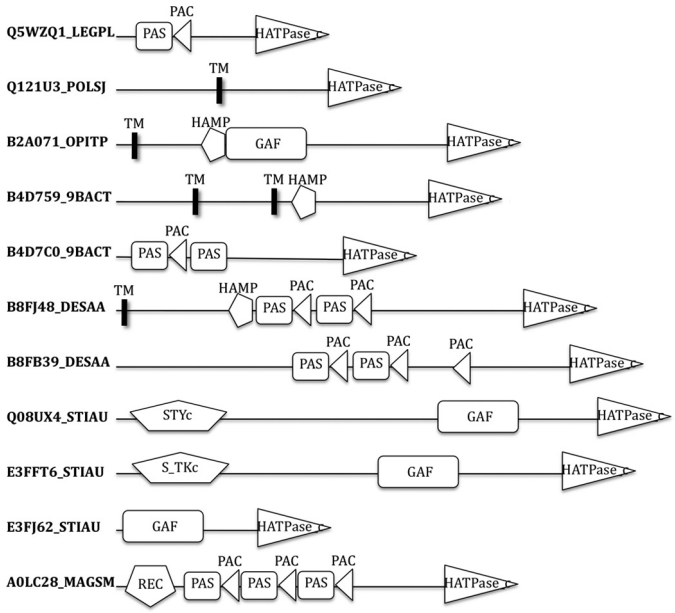

FIGURE 6. **Structural diversity within the HGN HK subfamily.** Graphic illustrations of domain arrangement of representative members of the HGN H box-containing HK are shown. PAS, PAC, GAF, or HAMP domain-containing structures still exist with or without transmembrane domains (half of the 65 HGN H box-containing proteins show no transmembrane domain). To simplify, only one version is shown. PAS, Per-Arnt-Sim domain; GAF, cyclic cGMP-specific and-regulated cyclic nucleotide phosphodiesterases, *Anabaena* adenylyl cyclase, and *E. coli* transcription factor *Fhl*A; HAMP, HK, adenylyl cyclase, methyl binding protein-phosphatase domain; STYKc, S_TKc, Ser/Thr kinase catalytic domains; TM, transmembrane domains.

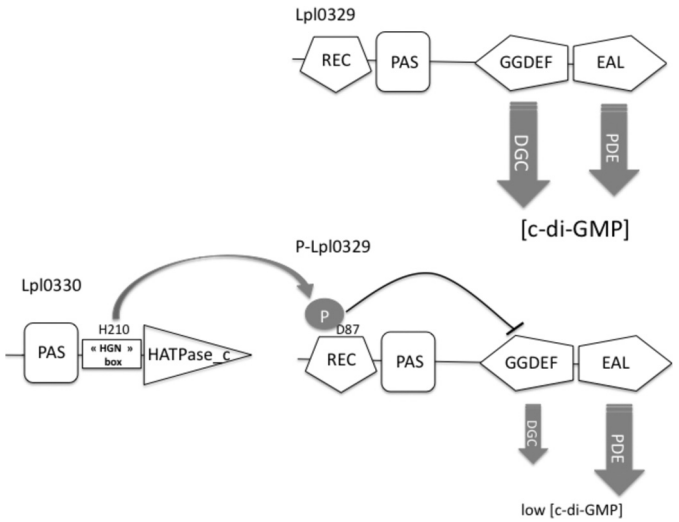

FIGURE 7. **Model for TCS Lpl0330/Lpl0329 control of c-di-GMP synthesis.** Lpl0329 is a bifunctional DGC/PDE enzyme. Phosphorylation of Lpl0329 by HK Lpl0330 leads to a decrease of DGC activity and thus modulates the local concentration of c-di-GMP.

Especially, 18 of the 24 species that contain the HGN H box can be found in all classes of Proteobacteria phylum (except alpha and zeta Proteobacteria). Most of proteins in this HK subfamily are associated with various sensor modules, such as PAS, PAC (PAS-associated C-terminal domain), GAF (cyclic cGMP-specific and-regulated cyclic nucleotide phosphodiesterases, *Anabaena* adenylyl cyclase, and *E. coli* transcription factor *Fhl*A), HAMP (HK, adenylyl cyclase, methyl-binding protein-phosphatase domain). Interestingly, seven proteins also contain Ser/Thr kinase catalytic domains (STYKc or S_TKc), which suggests that these proteins participate in hybrid-type signal phosphorelay (Fig. 6). The linkage of the HGN H box with a large variety of modules involved in signal sensing indicates that this HK family would participate in signal transduction pathways to respond to various external or internal signals. Moreover, *in silico* analysis of genome loci that contain the HK-encoding genes showed that the response regulators genetically linked to this HK subfamily are both transcriptional regulators and enzymatic proteins (data not shown). So, this HK subfamily would be involved in various signal transduction pathways to control different physiological functions.

The hypothesis according which the c-di-GMP biosynthesis could be regulated by two component systems has been recently introduced because 8.1% of all GGDEF/EAL proteins harbor a REC domain and thus could be identified as RR of a TCS (9). Moreover, two REC-GGDEF proteins, PleD and WspR, have been shown to be part of a two-component signal transduction pathway, and their functions have been demonstrated to depend directly on their phosphorylation and oligomerization states (34–37). In addition, one REC-EAL protein, VieA, has also been identified (38). However, to our knowledge, Lpl0329 is only the fourth demonstrated bifunctional DGC/PDE enzyme and the first example of phosphorylation-mediated molecular switch between these two opposite activities. It is noteworthy that 399 proteins harbor a REC domain in addition to the both GGDEF and EAL domains (P2CS data base) (25). According to our results, it is reasonable to anticipate that phosphorylation could participate to control activities of some of these proteins.

The HK Lpl0330 contains both heme binding PAS domain and HK domain, thus suggesting an oxygen-regulated signal-transducing system as for FixL/FixJ TCS, which is a paradigm for O_2 signal transduction (27). It has been shown that excess levels of O_2 inhibit FixL autokinase activity but have no effect on phosphoryl transfer from Phospho-FixL to FixJ (39). Contrary to FixL, in our normoxic conditions, Lpl0330 autophosphorylation seems effective and requires the presence of the PAS domain. However, we failed to detect a large amount of phosphorylated form of Lpl0329 in the presence of Lpl0330 and ATP. In many TCS, dephosphorylation of the P∼RR via the phosphatase activity of the HK limits the level of the activated RR and resets the system (31, 32). We propose that phosphoryl transfer from P∼Lpl0330 to Lpl0329 Asp-87 effectively occurs and that phosphatase activity of Lpl0330 rapidly hydrolyzes P∼Lpl0329. In this case, it would be interesting to explore whether hypoxic conditions increase P∼Lpl0329 level by enhancing or inhibiting Lpl0330 kinase or phosphatase activities, respectively.

Our data demonstrate that Lpl0329 phosphorylation leads to inhibition of the DGC activity (Fig. 7). So, Lpl0330/Lpl0329 proteins constitute an example of a TCS module integrated with a c-di-GMP control module. Regulation of Lpl0329 DGC/PDE activities is consistent with the necessity of a fine tuning of c-di-GMP synthesis and degradation, to ensure signal pathways efficiency, especially because DGC activity operates *in vivo* close to saturation (5) (the cellular concentration of the DGC substrate GTP is in the millimolar range) (40). Similar to HKs,

which exhibit both phosphoryl transferase and phosphatase activities to control the rate of P∼RR, bifunctional DGC/PDE enzymes such as Lpl0329 allow control of the signal rate, namely the c-di-GMP concentration, to modulate the associated signal transduction pathway.

In many RR transcription factors, phosphorylation mediates dimerization of the REC domains, which in turn facilitates DNA binding and transcription activation. A similar mechanism occurs in the two well studied RRs containing GGDEF domains (41). Phosphorylation promotes PleD dimerization (34, 36) and a dimer-tetramer transition in WspR (37). It should be noted that most GGDEF domains require dimerization to bring together two bound GTP molecules for the synthesis of c-di-GMP (36, 42) whereas dimerization of EAL domains does not seem to be systematically required for PDE activity (43). To investigate the impact of phosphorylation on the oligomerization state of Lpl0329, cross-linking and gel filtration assays with Lpl0329 in the presence or not of AcP which mimics the phosphorylated state were carried out (data not shown). A significant part of Lpl0329 homodimerizes *in vitro* even in the absence of phosphorylation as was described for the NtrC RR subfamily (41), and therefore it is unlikely that the oligomerization of Lpl0329 is strictly dependent on its phosphorylation. However, the phosphorylated state of the protein could cause structural rearrangement of the oligomers allowing a change in the enzymatic activity. A simple hypothesis would be that the phosphorylation of Lpl0329 leads to a conformational change that affects the proximity between the GTP binding sites of the two subunits of the dimers, without affecting PDE activity of the protein. The x-ray crystal structure of Lpl0329 in the presence of BeF_3^- to mimic the phosphorylated state, together or not with substrate analogs such as GTPαS, as has been done in the case of PleD (36), will undoubtedly be necessary to define the subtle domain arrangements in the structure and to validate our current hypothesis.

Acknowledgments—We thank Nathalie Baïlo and Claire Andréa for technical assistance.

REFERENCES

1. Stock, A. M., Robinson, V. L., and Goudreau, P. N. (2000) *Annu. Rev. Biochem.* **69,** 183–215
2. Hoch, J. A. (2000) *Curr. Opin. Microbiol.* **3,** 165–170
3. Gao, R., and Stock, A. M. (2009) *Annu. Rev. Microbiol.* **63,** 133–154
4. Galperin, M. Y., and Nikolskaya, A. N. (2007) *Methods Enzymol.* **422,** 47–74
5. Hengge, R. (2009) *Nat. Rev. Microbiol.* **7,** 263–273
6. Boehm, A., Kaiser, M., Li, H., Spangler, C., Kasper, C. A., Ackermann, M., Kaever, V., Sourjik, V., Roth, V., and Jenal, U. (2010) *Cell* **141,** 107–116
7. Fang, X., and Gomelsky, M. (2010) *Mol. Microbiol.* **76,** 1295–1305
8. Paul, K., Nieto, V., Carlquist, W. C., Blair, D. F., and Harshey, R. M. (2010) *Mol. Cell* **38,** 128–139
9. Seshasayee, A. S., Fraser, G. M., and Luscombe, N. M. (2010) *Nucleic Acids Res.* **38,** 5970–5981
10. Sommerfeldt, N., Possling, A., Becker, G., Pesavento, C., Tschowri, N., and Hengge, R. (2009) *Microbiology* **155,** 1318–1331
11. Brüggemann, H., Hagman, A., Jules, M., Sismeiro, O., Dillies, M. A., Gouyette, C., Kunst, F., Steinert, M., Heuner, K., Coppée, J. Y., and Buchrieser, C. (2006) *Cell Microbiol.* **8,** 1228–1240
12. Karatan, E., and Watnick, P. (2009) *Microbiol. Mol. Biol. Rev.* **73,** 310–347
13. Ryan, R. P., Fouhy, Y., Lucey, J. F., and Dow, J. M. (2006) *J. Bacteriol.* **188,** 8327–8334
14. Kumar, M., and Chatterji, D. (2008) *Microbiology* **154,** 2942–2955
15. Tarutina, M., Ryjenkov, D. A., and Gomelsky, M. (2006) *J. Biol. Chem.* **281,** 34751–34758
16. Ferreira, R. B., Antunes, L. C., Greenberg, E. P., and McCarter, L. L. (2008) *J. Bacteriol.* **190,** 851–860
17. Finn, R. D., Mistry, J., Tate, J., Coggill, P., Heger, A., Pollington, J. E., Gavin, O. L., Gunasekaran, P., Ceric, G., Forslund, K., Holm, L., Sonnhammer, E. L., Eddy, S. R., and Bateman, A. (2010) *Nucleic Acids Res.* **38,** D211–222
18. Fritsch, F., Mauder, N., Williams, T., Weiser, J., Oberle, M., and Beier, D. (2011) *Microbiology* **157,** 373–386
19. Christen, M., Christen, B., Folcher, M., Schauerte, A., and Jenal, U. (2005) *J. Biol. Chem.* **280,** 30829–30837
20. Wan, X., Tuckerman, J. R., Saito, J. A., Freitas, T. A., Newhouse, J. S., Denery, J. R., Galperin, M. Y., Gonzalez, G., Gilles-Gonzalez, M. A., and Alam, M. (2009) *J. Mol. Biol.* **388,** 262–270
21. Hickman, J. W., Tifrea, D. F., and Harwood, C. S. (2005) *Proc. Natl. Acad. Sci. U.S.A.* **102,** 14422–14427
22. Bordeleau, E., Brouillette, E., Robichaud, N., and Burrus, V. (2010) *Environ. Microbiol.* **12,** 510–523
23. Bouché, S., Klauck, E., Fischer, D., Lucassen, M., Jung, K., and Hengge-Aronis, R. (1998) *Mol. Microbiol.* **27,** 787–795
24. Ulrich, L. E., and Zhulin, I. B. (2010) *Nucleic Acids Res.* **38,** D401–407
25. Barakat, M., Ortet, P., Jourlin-Castelli, C., Ansaldi, M., Méjean, V., and Whitworth, D. E.(2009) *BMC Genomics* **10,** 315
26. Marchler-Bauer, A., Anderson, J. B., Chitsaz, F., Derbyshire, M. K., DeWeese-Scott, C., Fong, J. H., Geer, L. Y., Geer, R. C., Gonzales, N. R., Gwadz, M., He, S., Hurwitz, D. I., Jackson, J. D., Ke, Z., Lanczycki, C. J., Liebert, C. A., Liu, C., Lu, F., Lu, S., Marchler, G. H., Mullokandov, M., Song, J. S., Tasneem, A., Thanki, N., Yamashita, R. A., Zhang, D., Zhang, N., and Bryant, S. H. (2009) *Nucleic Acids Res.* **37,** D205–210
27. Gilles-Gonzalez, M. A., Gonzalez, G., Sousa, E. H., and Tuckerman, J. (2008) *Methods Enzymol.* **437,** 173–189
28. Dutta, R., and Inouye, M. (2000) *Trends Biochem. Sci.* **25,** 24–28
29. Altschul, S. F., Madden, T. L., Schäffer, A. A., Zhang, J., Zhang, Z., Miller, W., and Lipman, D. J. (1997) *Nucleic Acids Res.* **25,** 3389–3402
30. Wolanin, P. M., Thomason, P. A., and Stock, J. B. (2002) *Genome Biol.* **3,** REVIEWS3013
31. Russo, F. D., and Silhavy, T. J. (1993) *Trends Microbiol.* **1,** 306–310
32. Kenney, L. J. (2010) *Curr. Opin. Microbiol.* **13,** 168–176
33. Lukat, G. S., McCleary, W. R., Stock, A. M., and Stock, J. B. (1992) *Proc. Natl. Acad. Sci. U.S.A.* **89,** 718–722
34. Paul, R., Abel, S., Wassmann, P., Beck, A., Heerklotz, H., and Jenal, U. (2007) *J. Biol. Chem.* **282,** 29170–29177
35. Lai, T. H., Kumagai, Y., Hyodo, M., Hayakawa, Y., and Rikihisa, Y. (2009) *J. Bacteriol.* **191,** 693–700
36. Wassmann, P., Chan, C., Paul, R., Beck, A., Heerklotz, H., Jenal, U., and Schirmer, T. (2007) *Structure* **15,** 915–927
37. De, N., Navarro, M. V., Raghavan, R. V., and Sondermann, H. (2009) *J. Mol. Biol.* **393,** 619–633
38. Martinez-Wilson, H. F., Tamayo, R., Tischler, A. D., Lazinski, D. W., and Camilli, A. (2008) *J. Bacteriol.* **190,** 6439–6447
39. Gilles-Gonzalez, M. A., and Gonzalez, G. (1993) *J. Biol. Chem.* **268,** 16293–16297
40. Buckstein, M. H., He, J., and Rubin, H. (2008) *J. Bacteriol.* **190,** 718–726
41. Gao, R., and Stock, A. (2010) *Curr. Opin. Microbiol.* **13,** 160–167
42. Schirmer, T., and Jenal, U. (2009) *Nat. Rev. Microbiol.* **7,** 724–735
43. Schmidt, A. J., Ryjenkov, D. A., and Gomelsky, M. (2005) *J. Bacteriol.* **187,** 4774–4781
44. Larkin, M. A., Blackshields, G., Brown, N. P., Chenna, R., McGettigan, P. A., McWilliam, H., Valentin, F., Wallace, I. M., Wilm, A., Lopez, R., Thompson, J. D., Gibson, T. J., and Higgins, D. G. (2007) *Bioinformatics* **23,** 2947–2948
45. Crooks, G. E., Hon, G., Chandonia, J. M., and Brenner, S. E. (2004) *Genome Res.* **14,** 1188–1190